CFD Analysis of a Pressure Compensator for Variable Displacement Pumps

22nd Australasian Fluid Mechanics Conference AFMC2020
Brisbane, Australia, 7-10 December 2020
https://doi.org/10.14264/44f591d

CFD Analysis of a Pressure Compensator for Variable Displacement Pumps

M. Rundo[1] and P. Fresia[1]

[1]Department of Energy

Politecnico di Torino, Turin 10129, Italy

Abstract

In this paper a 3D CFD model of a three-port pilot valve for the displacement control of positive displacement pumps is presented. The model considers the spool radial clearance and the fillet radii of the metering edges. The valve was tested with imposed positions of the spool for measuring the modulated pressure and the control flow. The spool position was measured by means of a high accuracy contactless transducer. The model was used to determine the relationship between the valve discharge coefficients and the flow number. It was also found that cavitation occurs, leading to a reduction of the discharge coefficient. The developed 3D model can be used for tuning a 0D model of a pump displacement control.

Keywords

Hydraulic pump; displacement control; discharge coefficient.

Introduction

In positive displacement machines, such as piston or vane pumps, the flow rate can be continuously modified by means of a displacement control. In pumps with constant pressure compensators, a pilot valve modulates the pressure in a hydraulic actuator mechanically linked to the device for the displacement variation [1]. The system is closed loop controlled, where the linearized coefficients of the valve play the role of gains in the block diagram of the state variable model [2]. The valve design is crucial for both the steady-state and the dynamic performance of the control, in terms of accuracy, transient time and stability [3]. In a 0D model [4], the discharge coefficients of the valve are typically unknown parameters that must be tuned experimentally or by means of CFD simulations [5]. It was demonstrated that the values of such coefficients could discriminate between a condition of stability or instability [6]. Due to the small size of the valve, with flow rates in steady-state conditions lower than 1 L/min, an accurate measurement of the hydraulic characteristics is not an easy task, since the spool position must be determined with a very high precision. Moreover, even the manufacturing tolerances can affect the measurement. In this context, a reliable CFD model of the control valve represents the only solution for determining the discharge coefficients.

In literature recent examples of 3D models for the simulation of fluid power direction control valves developed with reliable commercial codes are available. Among the others, Lisowski and Filo [7] determined the relationship between the discharge coefficient and the spool position, while Tamburrano et al. [8] analysed the leakages between the spool and the sleeve in a servovalve with ANSYS Fluent®. The spin effect on the spool was simulated with PumpLinx® by Frosina et al. [9].

In the present study a 3D CFD model developed in FloEFD® is used for determining the discharge coefficients of a hydraulic valve for the displacement control of a piston pump. Both leakages and fillet radii of the spool are considered.

Component description

The hydraulic scheme of the displacement control used in the present study is shown in figure 1. The pump displacement depends on the equilibrium between the forces exerted by a spring and a hydraulic actuator. The configuration of maximum displacement is obtained when the actuator is connected to the atmospheric pressure and the only force acting on the swash plate is due to the spring. This condition occurs when the three-port valve is at rest and the port A is connected to port T.

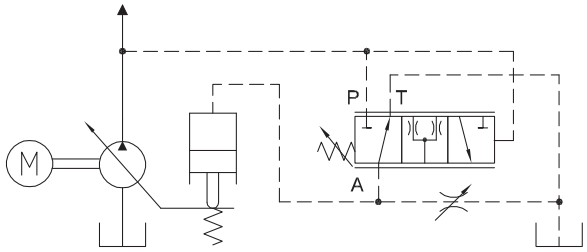

Figure 1. Hydraulic scheme of the displacement control.

When the delivery pressure achieves the setting of the adjustable spring, the spool translates, and the port A is progressively connected to P; at the same time, the flow area A-T is gradually reduced. The consequence is the increment of the pressure in the actuator and the reduction of the pump displacement. After the transient, an equilibrium position of the spool is established, corresponding to a specific value of the pressure in the actuator and of the pump displacement.

In figure 2 a section view of the pilot valve is reported: the lower side is connected to the pump casing, while in the upper side an additional control, not used in the current study, is housed. The flow areas are controlled by the lands 1 and 2 respectively for the connection P-A and A-T. The diameter of the holes and of the spool were measured with a resolution of 1 μm, while the distance between the external faces of the lands with a precision of 0.01 mm. Ideally, the entire modulation of the flow areas occurs with a spool stroke just higher than 0.1 mm.

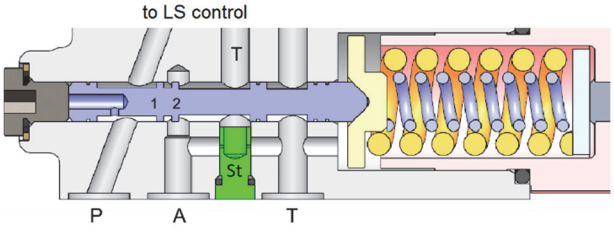

Figure 2. Section view of the control in the position at rest.

The delivery pressure acts always on the left side of the spool thanks to a radial and an axial hole, while the preload of the double spring can be adjusted by means of a screw.

The restrictors St (bleed), with diameter 0.65 mm, are drilled on a plug, whose position can be modified by means of a screwdriver. In the shown position the restrictors are open, while they are closed if the plug rotates by 90 degrees. The aim of the orifices is to modify the variation of the modulated pressure as function of the spool displacement, in order to avoid a possible instability.

CFD model

The 3D CFD model was built with the commercial tool FloEFD embedded in the CAD software Solid Edge®. The governing equations are discretised by means of the finite volume method. The code automatically determines the fluid volume when the boundary conditions are applied to an enclosed region; hence it is necessary to close all open ports by means of "lids". However, due to the very small flow area across the metering edges of the spool with respect to the diameter of the other holes, it is enough to limit the computational domain to the region around the lands 1 and 2. For this reason a specific CAD model of only the region of interest was created (figure 3). The model can be parametrized with respect to the spool position, the radial clearance spool-housing and the fillet radius of the lands and of the hole in the housing; for this last parameter a single value was assumed for all radii. In order to reduce the total amount of cells, the double symmetry with respect to the X and Y axes was exploited. Therefore, only the domain with the continuous line was analysed.

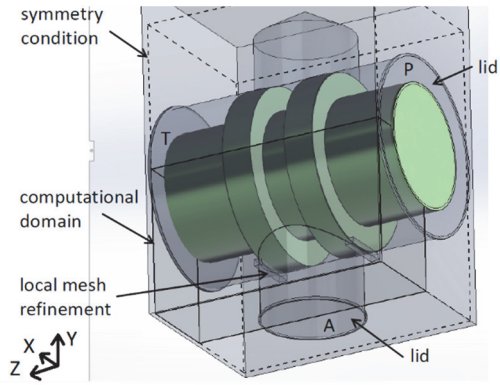

Figure 3. Simplified CAD model for the CFD simulations.

Two prismatic parts were superimposed to the assembly, but not considered in the definition of the fluid boundary, for defining regions with a finer grid across the metering edges. As boundary conditions, the static pressure was imposed on the lids at ports P and T, while at port A a wall condition was imposed, since a steady-state condition of the pump actuator is considered. The computational domain is visible in figure 4.

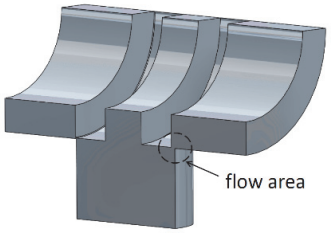

Figure 4. Computational domain with bleed orifice closed.

The general mesh is an unstructured Cartesian grid made by rectangular parallelepipeds, while the cells are cut on the boundaries. The code uses 2nd order spatial interpolation schemes, upwind for the convective terms and central for the diffusive terms. The Favre-averaged Navier-Stokes equations are implemented, with a low Reynolds k-ε Lam-Bremhorst model. In the near-wall regions a laminar/turbulent boundary layer model based on the Two-Scale Wall Functions (2SWF) approach is utilized; it uses two different methods depending on the number of cells across the boundary layer. For the pressure-velocity coupling, a method based on the SIMPLE approach is implemented. The isothermal cavitation model approach is used for the two-phase flow in a user-defined fluid. Basically, the density of the mixture is calculated as function of the pressure using a different linear relationship depending on the current state (liquid with dissolved gas, two-phase, only ideal gas) discriminated by the saturation pressure. The model was proved to be reliable in reproducing the choked flow in a nozzle [10].

Three nested regions were defined for the local refinement. In figure 5 the detail of a configuration with a radial clearance of 0.01 mm and fillet radii 0.02 mm is shown; for the illustrated position of the spool, the theoretical flow area should be completely closed, since there is an overlap between the land and the casing, however the flow area is not zero due to the real geometry of the spool (clearance and fillet radius).

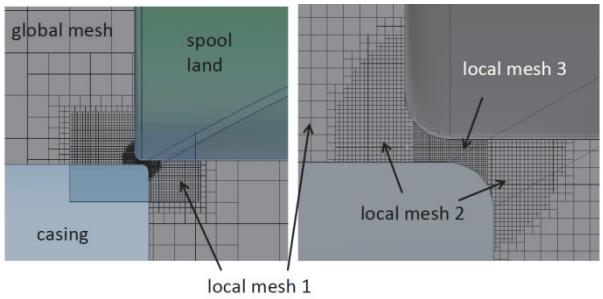

Figure 5. Mesh in correspondence of the metering edge with minimum flow area through the radial clearance.

The cells of the global mesh have a medium size of about 0.1 mm. In the local mesh 1 the cell sides are divided by 16, in the local mesh 2 by 64 and finally in the region 3 by 128, leading to a number of cells in the radial direction in correspondence of the clearance equal to 10, with size of the order of 1 μm. A mesh sensitivity analysis was performed for the case shown in figure 5. Two configurations with fewer cells and two with a higher number of cells were tested. The global mesh and the local mesh 1 remained unchanged, while in the regions 2 and 3 the cell size was further halved or doubled. In figure 6 the flow rate through the valve and the CPU time on an eight core Xeon HT processor at 3.4 GHz (8 physical cores used) are shown. It is evident that about 1 million represents the best compromise between accuracy and computational time.

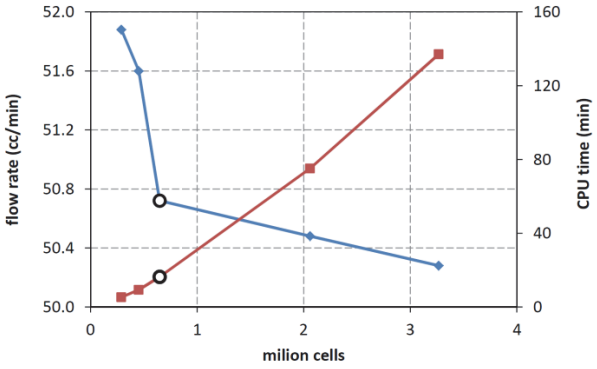

Figure 6. Flow rate and CPU time vs. number of cells.

Experimental facility

For validating the model, different positions of the valve spool were imposed and the corresponding flow rate and modulated pressure at port A were measured. The control was mounted on a test rig for servovalves fed by a constant pressure flow generation unit. The simplified scheme is reported in figure 7. The port A was closed: this condition is reasonable, since in steady-state conditions the displacement actuator of the pump is still, and the pressure A acts statically on its surface without a flow rate through it. The pressure at port P was set by a reducing valve VR. The valve springs were substituted by a metal spacer, maintained in contact against the spool by the pressure at port P; in this way, by rotating the screw it was possible to set the spool position.

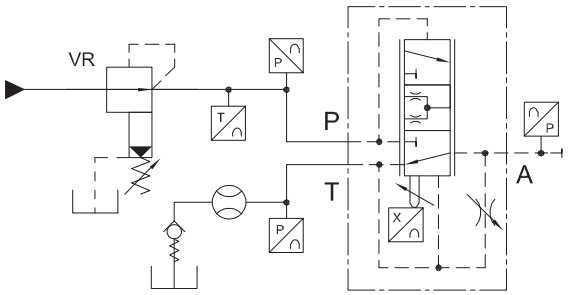

Figure 7. Layout of the test rig for the validation of the model.

The current spool displacement was detected by a contactless transducer KAMAN KD2300-1SUM with accuracy 0.1 µm and measuring range 1.25 mm. The transducer used as target the head of the screw for regulating the spool position. The flow rate through the valve was measured by a KEM ZHM02 gear flowmeter with measuring range 0.1-4 L/min connected at the port T. The pressure at port P was measured by a Danfoss MBS 3050 transducer, while the pressures at port T and A with transducers BELL & HOWELL BHL-4100. The temperature at port P was also monitored. All signals were acquired by a 12-bit NI data acquisition card PCI 6071E controlled by Virtual Instrument developed in Labview®.

Results and discussion

Two different types of test were performed: as function of the spool position with constant inlet pressure p_P at port P (50 and 100 bar) and with constant position of the spool as function of the pressure P. In the former case, by means of a wrench, the spool position was progressively modified with small steps of about 10 µm. Figures 8 and 9 show respectively the volumetric flow rate Q through the valve and the pressure at port A as function of the spool displacement with inlet pressure at port P equal to 100 bar and bleed orifice closed.

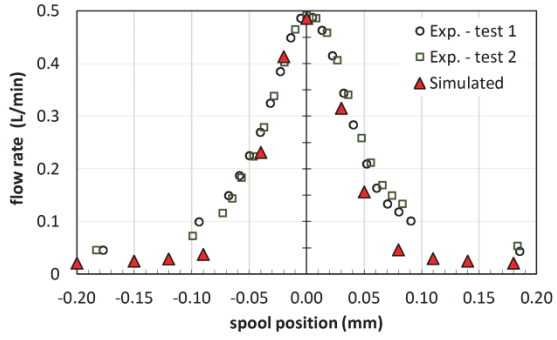

Figure 8. Flow rate vs. position with p_P = 100 bar, bleed closed.

Two repetitions of the experimental tests are reported for showing the good repeatability. The flow rate is also reported in figure 10 for the case with inlet pressure 50 bar.

Figures 11 and 12 show respectively the flow rate and the modulated pressure with bleed orifice open and inlet pressure equal to 100 bar. It is evident how the pressure modulation occurs with a longer stroke of the spool, leading to a reduction of the valve pressure gain. Even with this configuration, a good agreement was obtained with the experimental data.

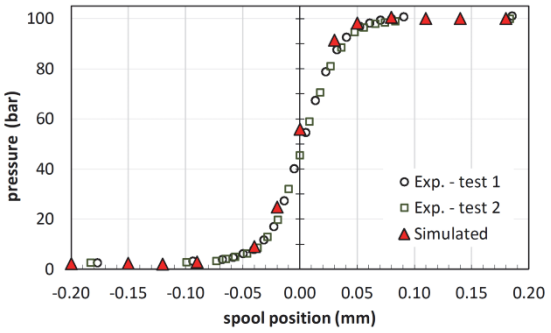

Figure 9. Pressure p_A vs. position with p_P = 100 bar, bleed closed.

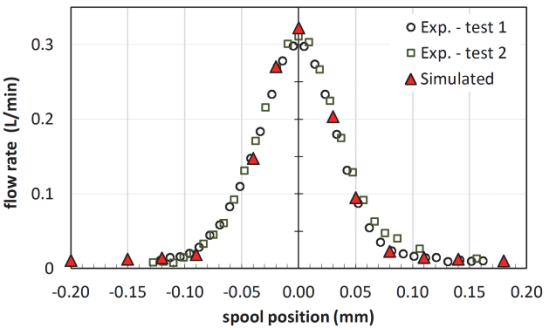

Figure 10. Flow rate vs. displacement with p_P = 50 bar, bleed closed.

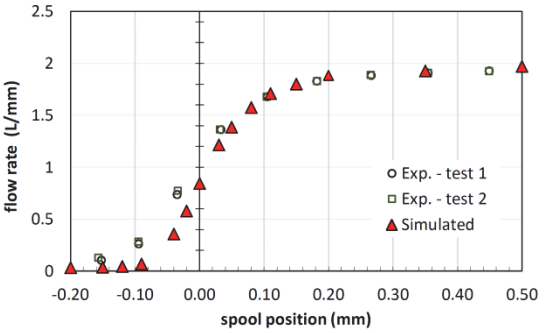

Figure 11. Flow rate vs. position with p_P = 100 bar, bleed open.

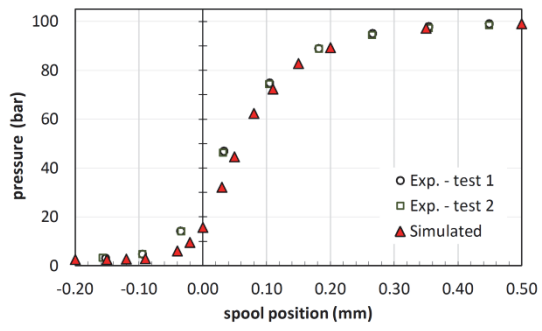

Figure 12. Pressure p_A vs. position with p_P = 100 bar, bleed open.

The validated model can be used for determining the discharge coefficients C_d of the valve in different operating conditions by means of the flow number λ defined as:

$$\lambda = \frac{d_h}{\nu}\sqrt{\frac{2\Delta p}{\rho}} \qquad (1)$$

being d_h the hydraulic diameter, ν the kinematic viscosity, Δp the pressure drop across the metering edge and ρ the fluid density. The discharge coefficient is calculated starting from the equation for turbulent regime:

$$C_d = \frac{Q}{A}\sqrt{\frac{\rho}{2\Delta p}} \qquad (2)$$

where A is the geometric minimum flow area that depends on the current position of the spool. For the sake of conciseness only the condition with the spool in the central position (same flow areas P-A and A-T) is reported. The flow area was calculated considering the rounded edges of the spool and of the casing. In order to obtain a variation of the flow number, the simulations were performed with different values of the pressure at port P. In figure 13 the experimental validation in terms of flow rate vs. pressure is shown. It is evident that better results are obtained if the cavitation is considered. In fact, without the cavitation, unrealistic absolute negative pressure values occur in the region just downstream from the minimum flow area A-T, leading to a higher overall pressure drop across the valve and hence to a higher flow rate.

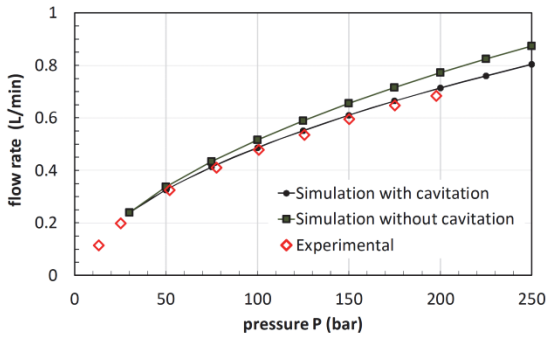

Figure 13. Flow-pressure characteristic with spool in central position.

Figure 14 shows the simulated relationship between C_d and λ for flow areas P-A and A-T. As expected, the discharge coefficient tends asymptotically to a maximum value corresponding to the condition of fully developed turbulent regime. However, the cavitation downstream of the flow area A-T generates a higher contraction of the jet that leads to a significantly lower coefficient. Consequently, also the modulated pressure will be affected, since even at equal flow areas the flow conditions through the valve are asymmetric.

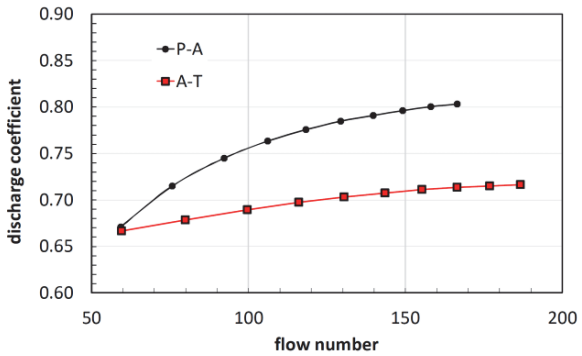

Figure 14. Discharge coefficients vs. flow number in central position.

The velocity field of the fluid jet through the metering edges for the condition with maximum working pressure of 250 bar is shown in figure 15. The cut plot was obtained using a plane passing through the axes of the spool and of the port A. The underlap of the spool for both sides is of the order of 65 µm.

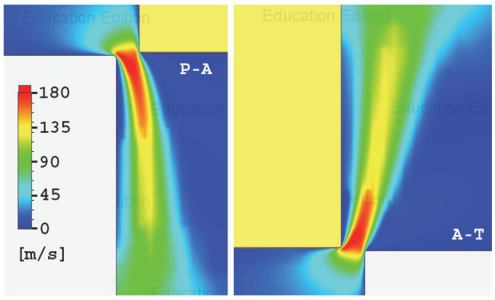

Figure 15. Velocity field in the flow areas P-A and A-T at 250 bar.

Conclusions

The discharge coefficients in a pilot hydraulic valve used in pump displacement controls can have a significant influence on the system performance. In this study a 3D CFD model of a pilot valve was developed and validated. A good agreement was found in all analysed operating conditions, as function of both the spool position and the inlet pressure. An important finding is that the valve behaviour is affected by the cavitation in correspondence of the outlet port, that leads to a reduction of the discharge coefficient. Although the developed model cannot be utilized directly for the simulation of the entire displacement control, a practical application is the tuning of the coefficients to be used in a lumped parameter model.

References

[1] Manring, N.D. and Johnson, R.E. (1996). Modeling and designing a variable-displacement open-loop pump. *J. Dyn. Sys., Meas., Control.*, 118(2), 267-271.

[2] Zeiger, G. and Akers, A. (1996). Dynamic Analysis of an Axial Piston Pump Swashplate Control. *Proc. IMechE, Part C: J. Mech. Eng. Sci.*, 200, 49-58.

[3] Mandal, N.P., Saha, R. et al. (2014). Pressure Compensator Design for a Swash Plate Axial Piston Pump. *J. Dyn. Sys., Meas., Control*, 136(2).

[4] Gilardino, L., Mancò, S. et al. (1999). An experience in simulation: the case of a variable displacement axial piston pump. *4th JHPS*, Nov. 15-17, Tokyo, Japan.

[5] Rundo, M. and Pavanetto, M. (2018). Comprehensive Simulation Model of a High Pressure Variable Displacement Vane Pump for Industrial Applications. *ASME IDETC/CIE*, Aug. 26-29, Quebec City, Canada.

[6] Fresia, P. and Rundo, M. (2020). Lumped Parameter Model and Experimental Tests on a Pressure Limiter for Variable Displacement Pumps. *75th ATI Conference*, Sept. 15-16, Rome, Italy.

[7] Lisowski, E and Filo, G. (2017). Analysis of a proportional control valve flow coefficient with the usage of a CFD method. *Flow Meas. Instrum.*, 53, 269-278.

[8] Tamburrano, P., Plummer, A.R., et al. (2019). Internal leakage in the main stage of servovalves: An analytical and CFD analysis. *AIP Conference Proceedings* 2191.

[9] Frosina, E., Senatore, A., et al. (2016). A Mathematical Model to Analyze the Torque Caused by Fluid-Solid Interaction on a Hydraulic Valve. *J. Fluids Eng.* 138(6).

[10] Dumnov, G., Muslaev, A. et al. (2013). Cavitation Process Simulation for Automotive Applications with an Isothermal Solver Approach. SAE paper 2013-01-1608.